PET Performance Measurements for an LSO-Based Combined PET/CT Scanner Using the National Electrical Manufacturers Association NU 2-2001 Standard

Yusuf E. Erdi, DSc[1]; Sadek A. Nehmeh, PhD[1]; Tim Mulnix, PhD[2]; John L. Humm, PhD[1]; and Charles C. Watson, PhD[2]

[1]*Department of Medical Physics, Memorial Sloan-Kettering Cancer Center, New York, New York; and* [2]*CPS Innovations, Knoxville, Tennessee*

Results of performance measurements for a lutetium oxyorthosilicate (LSO)-based PET/CT scanner using new National Electrical Manufacturers Association (NEMA) NU 2-2001 standards are reported. **Methods:** Performance measurements following the NU 2-2001 standards were performed on an LSO-based PET/CT scanner. In addition, issues associated with the application of the NEMA standard to LSO-based tomographs in the presence of intrinsic radiation are discussed. **Results:** We report on some difficulties experienced in following the suggested NEMA measurement techniques and describe alternative approaches. Measurements with the new standard (as compared with NU-1994) incorporate the effects of activity outside the scanner and facilitate measurements of the entire axial field of view. Realistic clinical conditions are also simulated in image quality measurements of a torso phantom. **Conclusion:** We find that, with appropriate modifications, NU 2-2001 can be successfully applied to LSO-based scanners.

Key Words: National Electrical Manufacturers Association; acceptance testing; PET/CT

J Nucl Med 2004; 45:813–821

The recent introduction of PET/CT scanners using lutetium oxyorthosilicate (LSO) scintillator detectors has made it possible to perform total-body oncologic scans in shorter periods than with bismuth germinate (BGO)-based scanners, as a result of the shorter decay time and higher light output of LSO. Cameras using this new scintillator can provide whole-body scans in less than 20 min, with the possibility in the near future of doing scans in less than 5 min (*1*,*2*). To ensure the quality of scans on these LSO systems, as well as to determine optimal system operation parameters, it is important to be able to characterize their performance in a reproducible and reliable manner according to accepted measurement standards.

The National Electrical Manufacturers Association (NEMA) has updated their standard PET performance measurement recommendations. The updated document (NU 2-2001) includes revised measurements for spatial resolution, scatter fraction, sensitivity, counting rate performance, and the accuracy of count loss and randoms corrections (*3*). This NU 2-2001 document also includes a specification for a new image quality measurement that was not considered in the original NU 2-1994 standard (*4*). Because of the prevailing interest in clinical whole-body scanning, this measurement is intended to simulate realistic clinical conditions for such scans. A recent publication by Daube-Witherspoon et al. (*5*) discussed in detail the performance measurements of several PET cameras using the new NU 2-2001 standards.

A brief introduction of each NU 2-2001 test will be followed by results of those tests for an LSO PET/CT scanner (CPS Innovations; marketed as the Reveal RT by CTI, Inc., and as the Biograph LSO by Siemens Medical Solutions). Other sources provide more details, and users wishing to perform the measurements described here are strongly encouraged to consult those publications for a complete description of procedures (*3*,*5*). However, it is not possible to follow all of these procedures exactly on LSO systems because of the presence of intrinsic background radiation in the detectors.

LSO contains natural lutetium, of which the radioactive nuclide ^{176}Lu composes 2.6%. The background single-event counting rate resulting from this activity depends on the details of the detectors' construction and energy discrimination settings. This rate is typically on the order of 1 million counts per second (cps) in the whole scanner, for a 350- to 650-keV acceptance win-

Received May 21, 2003; revision accepted Nov. 24, 2003.

For correspondence or reprints contact: Yusuf E. Erdi, DSc, Department of Medical Physics, Memorial Sloan-Kettering Cancer Center, New York, NY 10021.

E-mail: erdiy@mskcc.org

dow, which corresponds to a total random coincidence rate of about 1,600 cps. Singles rates in clinical acquisitions are generally 10–20 times higher. Noting that randoms increase approximately as the square of the singles rate (neglecting counting losses), the main effect of the intrinsic events is to increase the rate of random coincidences in the scanner by a few percent in the clinical range (about 8% at peak noise equivalent counting rate [NECR]). There is also a small (approximately 600 cps) background of true coincidences resulting from the intrinsic radiation, which may be compared with typical clinical trues rates of several hundred thousand counts per second. An intrinsic true event may result when a ^{176}Lu nuclide undergoes β-decay in one detector, depositing energy locally in that detector, and also emits a prompt γ-ray that is absorbed in a second detector.

The benefits of the short decay time and high light output of LSO strongly outweigh the deleterious effects of the intrinsic radiation on the counting rate performance of the CPS LSO PET/CT. Nevertheless, one must properly account for the intrinsic contribution when performing the NEMA tests. It is not possible, for example, to achieve a randoms-to-trues ratio of less than 1% in the counting rate test as specified by the NEMA standard. Consequently, one cannot accurately determine the scatter fraction according to its prescription. In another example, the small intrinsic trues contribution must be accounted for when the sensitivity test is performed with a weak source. For these reasons, we have not followed exactly or in all cases the NEMA NU 2-2001 specifications for experimental technique and data processing. Instead, we have implemented the suggestions for adapting the NEMA protocols to LSO systems discussed in some detail by Watson et al. (*6*). These refined procedures preserve the intent of the NEMA standards but properly account for aspects of the special nature of LSO cameras not addressed in NU 2-2001.

MATERIALS AND METHODS

PET/CT System

The CPS LSO PET/CT is a combined system that integrates a PET scanner (based on the CPS ECAT ACCEL) with a spiral CT scanner (SOMATOM Emotion; Siemens Medical Solutions) using the *syngo* multimodality computer platform (Siemens Medical Solutions). The SOMATOM Emotion is a dual-slice CT scanner and can acquire images with slice thicknesses from 1 to 10 mm. Minimum rotation time is 0.8 s per 360°. Tube current can be varied between 30 and 240 mA, and tube voltage settings are 80, 110, and 130 kV(p). The table feed rate of the CT scanner is from 1 to 25 mm per 360° rotation of the x-ray tube. Maximum scan time per spiral is 100 s. Reconstructed spatial resolution is 0.32 mm. The PET component of the tomograph has no septa and is a 3-dimensional (3D)-only scanner. It has 24 crystal rings with 384 crystals per ring. The size of each crystal is 6.45 × 6.45 × 25 mm, and the axial field of view (FOV) is 16.2 cm. The coincidence time window is set to 6 ns, taking full advantage of the short decay time and high light output of LSO. Such a short coincidence time window allows a random rate reduction by about a factor of 2 compared with BGO-based systems. The energy discrimination window was 350–650 keV for all measurements reported here.

Test Phantom Set and Activity

The NEMA NU 2-2001 tests require 3 sets of phantoms. First is an International Electrotechnical Commission (IEC) body phantom set, which consists of a torso cavity, removable lung insert, and 6 spheres (10–37 mm in inner diameter [ID]). All are fillable. Second is a scatter phantom set, including a solid circular cylinder composed of polyethylene with a specific gravity of 0.96, an outside diameter of 203 mm, an overall length of 700 mm, and a plastic tube that is 800 mm long and has an ID of 3.2 mm to hold the source activity. A sensitivity phantom set is the third required and consists of 5 concentric aluminum tubes (each 70 mm long) and a 1.8-mL fillable polyethylene tube inserted into the center sleeve. These NEMA phantoms were manufactured by Data Spectrum Corp. and marketed by Biodex Medical Systems. Detailed information and specifications for the NEMA NU 2-2001 phantoms can be found at www.biodex.com. As specified by NU 2-2001, all measurements were performed with the ^{18}F isotope.

Spatial Resolution

This measurement requires the construction of a point source. NU 2-2001 specifies that the activity be contained in a glass capillary tube with an ID less than 1 mm and that the tube also have an axial extent of less than 1 mm. It is further required that the source (i.e., tube) be placed parallel to the long axis of the tomograph for all measurements. We found this technique problematic for several reasons. The small volume of the source (<0.785 mm^3) necessitates a very high specific activity to get a reasonable counting rate. It is difficult to accurately draw up this amount of fluid without wetting the walls of the capillary beyond the desired region. Moreover, positron annihilation is not confined to the location of the ^{18}F in the fluid; positrons may stream up the capillary and annihilate in the glass of the tube. This positron range effect may tend to elongate the source in the direction of the tube. In our attempts at following the prescribed procedure, we measured significantly wider axial resolution when such a source was placed axially than when it was placed transaxially in the scanner, suggesting that the source was indeed asymmetric.

Consequently, we have followed a slightly different procedure for fabricating a point source. A small amount of ion exchange resin was placed in a small plastic tube (about 5 mm in length with an ID of 1 mm and outer diameter [OD] of 2 mm). Light packing material was placed in the tube on either end to hold the resin in place with an axial extent of less than 1 mm, and the tube was placed in a capsule that allowed it to be coupled to a syringe. These sources were manufactured by D and W, Inc. Approximately 300 MBq of $^{18}F^-$ ion in 2 mL of water were then flushed 3 times through the resin, followed by a rinse with approximately 50 mL of nonradioactive water. This resulted in an activity of 1.7 MBq residual in the resin. The plastic tube containing the resin was removed from the capsule and placed on a piece of tape, which was then suspended from a needle in the FOV of the scanner (Fig. 1A). Two complete sets of resolution measurements were made with this source, one with the axis of the tube parallel to the axis of the scanner and one with it perpendicular. Although both sets of results are

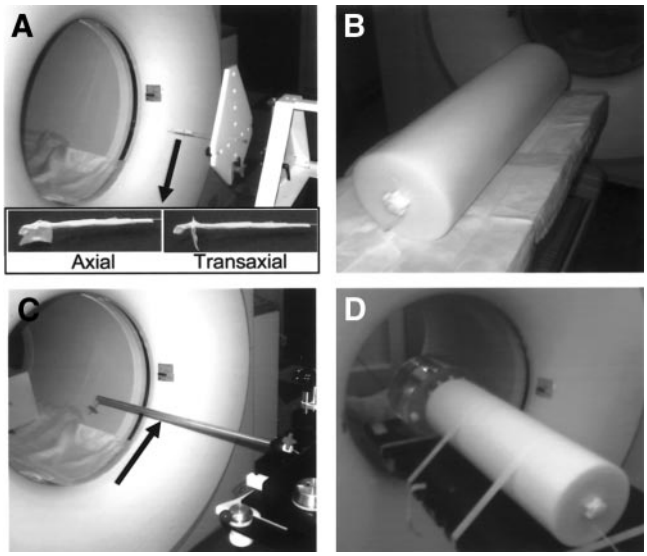

FIGURE 1. (A) Setup for axial and transaxial measurement. The point source was suspended from a needle in either an axial or a transaxial orientation, as shown in the insets. A template was used to position the point source for improved accuracy. (B) Scatter phantom with an embedded line source on the table. The acquisitions started at 740 MBq in the line source and continued for more than 8 half-lives (~15 h). This experiment yielded data for counting rate performance and scatter fraction. (C) Location of the line source for the sensitivity measurement (arrow). Tubes were pulled out from the back of the scanner after each measurement. In addition to the center, the measurement was repeated at a 10-cm radial offset by raising the table. (D) Image quality measurement. Four smaller spheres in the IEC body phantom and the background showed activity. Activity was also present in the form of a line source in the scatter phantom.

reported, we believe that the axial resolution measurements are more accurate for the transaxially oriented source and that the transverse resolution measurements are more accurate for the axially oriented source.

For each source orientation, the resolution measurements were made at 6 locations: 3 at the center of the axial FOV and 3 at positions corresponding to one fourth of the axial FOV from the center toward the patient table. For both those axial locations, the source was imaged at positions (a) $x = 0$ and $y = 1$ cm, and (b) $x = 0$ and $y = 10$ cm, and $x = 10$ and $y = 0$ cm. At each position, more than 2 million counts were acquired to ensure adequate statistics. These data were reconstructed and analyzed using the software tools provided by the manufacturer. The reconstruction and analysis of data conformed to the requirements of the NU 2-2001 specifications. Sinograms were rebinned axially using the Fourier rebinning (FORE) algorithm, followed by filtered backprojection (FBP) reconstruction.

Intrinsic Scatter Fraction

Scatter fraction is the ratio of scattered events to the sum of true (unscattered) and scattered events, excluding randoms. The NU 2-2001 procedure specifies that the scatter fraction be measured as part of the counting rate performance test, which is used to acquire prompt coincidence data only (trues plus scatter and randoms), under the assumption that low-activity frames contain negligible randoms (*3*). However, for LSO-based detectors such a randoms-free regime does not exist. Consequently, if the NEMA prescription were followed in this case it would result in a significant overestimate of the scatter fraction and a very inaccurate estimate of the randoms. A more accurate approach would be to directly measure the random event rate together with the prompts. From these data the scattered event rate can be estimated very accurately as a function of activity by subtracting the measured randoms and trues event rates from the total event rate (*6*). The standard NEMA procedure neglects the counting rate dependence of the scatter fraction.

Therefore, for the scatter fraction, count losses, and randoms measurement, separate prompt and delayed sinograms were acquired using a standard delayed coincidence window technique. Activity was injected into the line source (800-mm length, 3.2-mm ID, 4.8-mm OD, ~6-mL fillable volume), and the line source was threaded through the 6.4-mm hole in the test phantom (Fig. 1B). The test phantom was placed so that the line source was at the position nearest the patient table and was centered within 5 mm in the transverse and axial FOV.

Data analysis followed the modified procedure described elsewhere (*6*). Instead of estimating the randoms (R_r) from the prompts sinogram by correcting the totals (R_{TOT}) for trues (R_t) and scatter (R_s), these were computed directly from the delayed window sinogram using the same bins used for the analysis of the prompts sinogram. The scatter event rate for each slice (i) at each activity (j) was then computed from:

$$R_{s,i,j} = R_{TOT,i,j} - R_{t,i,j} - R_{r,i,j}, \qquad \text{Eq. 1}$$

neglecting the small intrinsic trues contribution, and the scatter fraction (SF) was estimated simply as:

$$SF_{i,j} = \frac{R_{s,i,j}}{R_{t,i,j} + R_{s,i,j}}. \qquad \text{Eq. 2}$$

Sensitivity

The sensitivity of a PET scanner is defined as the rate of true coincidence counts per second and per unit radioactivity that are detected for a line source located within the scanner FOV in the absence of attenuating media. To obtain an attenuation-free estimate, successive measurements are made with a uniform line source surrounded by a varying number of known absorbers. The absorbers consist of a set of nested, concentric aluminum tubes. Extrapolation of the response to 0 absorption gives an attenuation-free estimate of sensitivity. A 700-mm portion of the plastic tubing was filled with ~2.0 MBq of ^{18}F, a sufficiently low activity to ensure that counting losses were less than 1%. At this activity level, however, the true event rate was on the order of 10^4 cps, low enough that the intrinsic trues from the LSO itself (about 600 cps) were not negligible and required correction. For this purpose, a separate background scan was acquired with no phantom or activity present, and the total measured intrinsic trues rate was subtracted from the phantom data before computing the sensitivity (*6*).

After activation, the tube was suspended in the center of the transaxial FOV (Fig. 1C), parallel to the axis of the scanner, with all the absorbers in place. To help equalize counting rates as the source decayed, the measurement was started with all the aluminum tubes on the phantom. After each acquisition, a tube was pulled out and the measurement was repeated. More than 2 million counts were acquired with each configuration to ensure at least 10,000 trues per slice. The acquisitions were performed

in the default energy window, which was 350–650 keV. The same measurements were repeated at a 10-cm radial offset from the center of the transaxial view. Analysis of the data was performed according to NU 2-2001, using software supplied by the manufacturer.

Counting Rate Performance

To understand the scanner's performance under a wide range of imaging conditions, it is necessary to measure its behavior as a function of counting rate. For this purpose the 70-cm polyethylene cylinder with a line source threaded through along its length was used (the same measurement as for the scatter fraction determination previously outlined). NU 2-2001 specifies that the initial amount of radioactivity shall be such as to cause the true event rate to reach 50% dead-time loss value. However, on LSO-based scanners, detector dead time is so low that a 50% loss is not observed until the communications channel of the coincidence processor saturates. With the present generation of electronics, this occurs at a total coincidence rate of about 2.6 million events per second, well beyond the clinical regime and peak NECR of the scanner. Nevertheless, this saturation regime was included in the test reported here.

Following the suggestion of the manufacturer, the line source was filled with 740 MBq of ^{18}F initial activity, enough to achieve counting rates well beyond both the peak trues and the peak NECRs. Thirty-five frames were acquired, each with a 10-min duration, followed by a 15-min gap between the scans. Data were acquired over 15.5 h, and each acquisition had more than 3.3 million coincidence counts. In the analysis, the same process as described for intrinsic scatter fraction (delayed window sinogram) was used to account for randoms resulting from the intrinsic radioactivity of LSO.

Accuracy of Corrections for Count Losses and Randoms

PET scanners must be able to compensate for dead-time losses and randoms to achieve quantitative clinical measurements. Inaccuracy of corrections, especially at high counting rates, can cause bias in clinical scanning results. Thus it is important to measure the accuracy of the corrections for count losses and randoms. For this purpose, the counting rate data described previously were reconstructed with standard corrections and the FORE with ordered-subset expectation maximum (OSEM) iterative algorithm (2 iterations, 8 subsets). The counting rate error (Δr) as a function of effective activity concentration was calculated as the deviation of the trues from a linear trend extrapolated from low-activity acquisitions where dead-time losses were negligible. Details of the analysis are available in the NEMA standard (*3*).

Image Quality Measurement

An image quality measurement has been incorporated into the NEMA testing scheme to better compare the quality of different imaging systems for a standardized situation that simulates clinical conditions. According to NU 2-2001, the large background region of the IEC body phantom is to be filled with an activity of 5.3 kBq/mL. Activated and nonactivated spheres of various sizes are placed in this warm background. The hot spheres (10, 13, 17, and 22 mm in diameter) are to be filled with an activity concentration of n times that of the background, where $n = 4$ and 8. The 2 largest spheres (28 and 37 mm) are filled with water only. A 5-cm-diameter cylindric insert with a density approximately equal to the average value in lung tissue (0.30 g/mL) is to be placed in the center of the phantom. For the measurements reported here, however, this cylinder, which was packed with foam beads, was inadvertently left dry, and thus had a mean density of only 0.025 g/mL. This provided a somewhat more stringent test of attenuation and scatter correction than was intended, but the CT-based attenuation correction appeared to work quite well for this configuration, with no observable artifacts. Activity is also present outside the FOV of the scanner in the form of a line source in the scatter phantom, which is placed adjacent to the body phantom on one side. Its effective specific activity should be the same as that of the main chamber of the body phantom.

The intention of this measurement is to produce and evaluate images approximating those obtained in a whole-body study with both hot and cold lesions. The background activity level in the torso cavity is supposed to represent the level one would have in a patient weighing 70 kg after an injection of 370 MBq of ^{18}F-FDG (although no allowance is made for uptake time or excretion of part of the dose) (*3*). In our experience, however, the NECR of this phantom at a given activity concentration was not similar to that found in patients (*7*,*8*). The phantom's NECR peaked at a much higher value and at a much higher activity concentration than for average patients, probably as a result of the higher concentration of activity in the scanner's FOV and perhaps lower attenuation than in patients. Thus, at the specified 5.3 kBq/mL, the NECR for this study was significantly higher than would typically be achieved in patients but significantly lower than the maximum that could be achieved for this phantom. It is arguable, then, that this test may capture neither typical clinical performance nor the optimal performance of an LSO PET/CT. Nevertheless, we present measurements made at close to the recommended levels.

The actual specific activities we achieved are listed in Table 1. It must be acknowledged that there are relative uncertainties in these assays, which we believe are on the order of $\pm$5%. The hot-sphere contrast ratios depend on the relative accuracy of these assays and thus will exhibit corresponding uncertainties.

The setup for the image quality measurement can be seen in Figure 1D. Data were acquired on 2 consecutive days ($n = 4$ on day 1; $n = 8$ on day 2). Data acquisition time was determined considering the 12-cm (16 cm − 4 cm overlap) axial distance between consecutive bed positions in a total-body study. The imaging time was set to simulate a total-body scan (100-cm total axial imaging distance in 60 min). Because the transmission scan in the LSO PET/CT is performed with a 2-slice CT scanner, the contribution of the transmission scan into the total imaging time is

TABLE 1
Activity Concentrations for Image Quality Measurement

Area measured	Activity concentration	
	4:1 (kBq/mL)	8:1 (kBq/mL)
Background	4.78	5.66
Hot spheres	19.05	46.20
Scatter phantom ratios	3.82	5.53
Assayed hot-to-background ratio	3.99	8.17

negligible. Our calculation for the total scan time per bed position ($T_{T,E}$) yielded:

$$T_{T,E} = (60 \text{ min/distance}) \times \text{axial step}$$
$$= (60/100) \times 12$$
$$= 7.2 \text{ min.} \quad \text{Eq. 3}$$

Based on equation 3, we used 7 min for the emission scan and 0.2 min for the CT and positioning scan. Although this conforms to the NU 2-2001 specification, it should be noted that in our clinic patient scan times for the emission acquisitions on an LSO PET/CT scanner range from 1 to 5 min per bed position, depending on patient weight and part of the body scanned, and whole-body acquisitions never require 60 min.

Data acquired were reconstructed with all corrections using the available clinical reconstruction software. NU 2-2001 specifies that results be reported for "standard" reconstruction parameters. However, the CPS LSO PET/CT offers users a wide choice of reconstruction algorithms and parameters, and different clinics prefer different standards. For this reason, we report results for 3 different reconstructions: one FBP (unwindowed) and 2 using OSEM iterative reconstruction, with either 2 iterations and 8 subsets or 4 iterations and 16 subsets. In all cases, FORE was used to reduce the 3D dataset to 2-dimensional, and a 5-mm full-width-at-half-maximum (FWHM) gaussian filter (axial and transaxial) was applied to the image after reconstruction. Image size was 256 × 256, pixel size was 1.77 mm, and the slice thickness was 3.375 mm. To measure the residual error in scatter and attenuation corrections, the relative error ($\Delta C_{lung,i}$) in percentage units was calculated for each slice (i) by taking the ratio of the average counts in the lung insert ROI to the average counts in the background ROIs. For the analysis of image quality and accuracy of scatter and attenuation corrections, we have followed the guidelines presented in the NU 2-2001 protocol.

NU 2-2001 suggests that the image quality measurement may be repeated and that the results can be averaged to achieve more precise results. We were concerned particularly with the repeatability of the contrast measurement. Rather than repeating scans at approximately the same activity level, we instead performed repeated scans over a range of activity levels for the $n = 8$ case, to assess the effect of image noise level on contrast measurement. The measured activity levels were 2.3, 1.0, 0.46, and 0.20 times the standard background activity level. For this study, only FBP reconstruction was used. The relative standard deviations of the contrast values across the activity range were computed.

RESULTS

Spatial Resolution

The results for transaxial and axial resolutions are given in Table 2 for both the FWHM and full width at tenth maximum (FWTM). Values are presented for both orientations of the source, with the preferred values highlighted in bold. In fact, for this point source construction, only a few tenths of a millimeter difference could be seen in the 2 orientations. Both the axial and the transaxial FWHM resolutions degraded by about 1 mm in moving from 1 to 10 cm from the central axis of the scanner. The loss of resolution at FWTM was about 0.6 mm in the transverse direction and 1.6 mm axially, probably as a result of the effect of axial rebinning.

Intrinsic Scatter Fraction

Intrinsic scatter fraction measured at low activity levels was 47%. Scatter fraction may increase slightly as the activity increases, probably as a result of pile-up effects in the detectors. The system scatter fraction corresponding to the peak NEC activity ($a_{NEC,peak} = 14.7$ kBq/mL) is 48%.

Counting Rate Performance

Peak true counting rate was measured as 171 kcps at an activity concentration level of 21 kBq/mL. Peak NECR was 44.4 kcps at 14.7 kBq/mL for noiseless randoms correction and 31.4 kcps at 12.6 kBq/mL for online randoms subtraction. A plot of the trues, randoms, and NECRs versus activity is shown in Figure 2. It is important to realize that peak NECR occurs at lower activity concentrations in patients than it does in this phantom (*8*); thus, it is not accurate to infer optimal patient injected doses directly from these results. Counting rate analyses on clinical data on the LSO PET/CT scanner showed that peak NECR in an average adult patient weighing 70 kg was achieved with a mean activity concentration (assuming no excretion) of 6.7 kBq/mL (*7*).

Sensitivity

The total sensitivity values for radial positions of 0 and 10 cm were 6.1 and 6.5 kcps/MBq (0.61% and 0.65%), respectively. The dead-time loss during the measurement was less than 1%. A small intrinsic trues correction has been applied, as discussed previously. Because sensitivity is ex-

TABLE 2
Spatial Resolution Values

Distance (cm)	Direction	Description	FWHM* (mm)		FWTM* (mm)	
			Axial	Transaxial	Axial	Transaxial
1	Transverse	Average x and y for both z	**6.3**	6.6	**12.4**	13.0
1	Axial	Average for both z	6.1	**5.8**	12.3	12.0
10	Transverse radial	Average 2 transverse for both z	**7.4**	7.1	**13.0**	12.5
10	Transverse tangential	Average 2 transverse for both z	**6.8**	6.9	**13.1**	13.3
10	Axial resolution	Average 2 transverse for both z	7.0	**6.8**	13.9	**13.6**

*Measures refer to the orientation of the point source. Preferred values are in bold type.

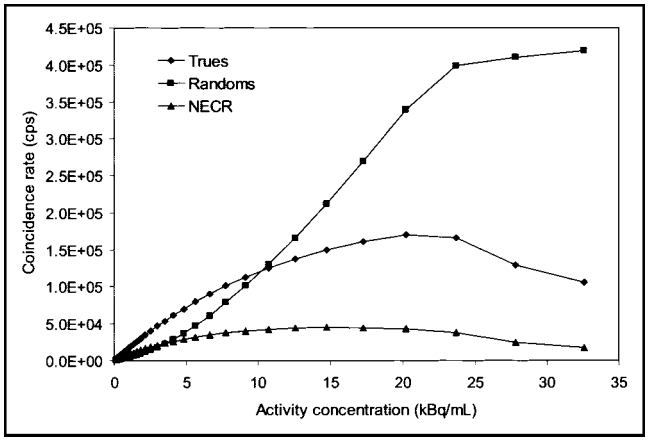

FIGURE 2. Trues, randoms, and NECRs observed during the counting rate test.

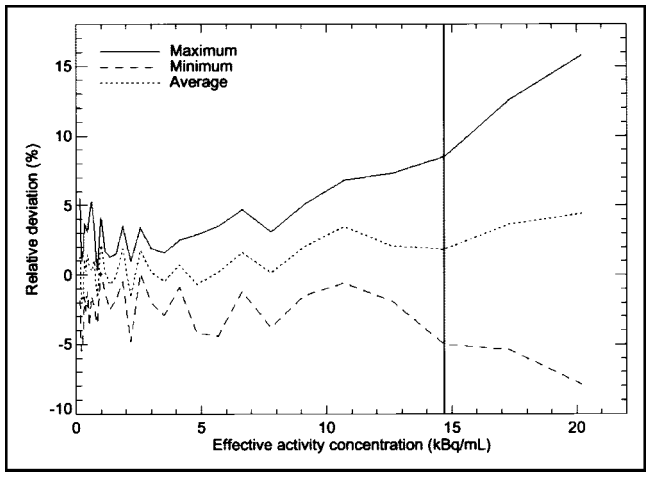

FIGURE 4. For each acquisition (j), the highest and lowest values of the relative counting rate error ($\Delta r_{i,j}$) over each slice (i), in percentage units. The vertical line indicates the level of $a_{NEC,peak}$ (14.7 kBq/mL) activity. At this activity level the maximum bias is less than 8.5%.

pressed as the rate of coincidence events per unit activity in the line source, it should be noted that a scanner with a shorter axial FOV would have a lower value than a system with a longer FOV, which would cover more of the line source (*5*). The axial FOV in the LSO PET/CT scanner is 162 mm. The axial sensitivity profile of the system is shown in Figure 3 for the source at the center and at 10 cm off axis.

Accuracy of Corrections for Count Losses and Randoms

The plot in Figure 4 shows the relative counting rate error in percentage points for the highest and lowest values among the slices versus the average effective activity concentration (a_{eff}), obtained by dividing the total activity present by the phantom's volume. Data corrections are not designed to work above the saturation point of the scanner, so we reported values only over the meaningful range, which is ~21 kBq/mL or less. Although the intention of this measurement is to determine accuracy, not precision, it seems clear from the fluctuations of the deviations, as well as the symmetry between positive and negative values, that there remains a large element of statistical uncertainty in these results, probably because of the difficulty in determining the precise linear trend, despite the fact that the NU 2-2001 specification was followed here. Therefore, we also showed the average deviation versus a_{eff} in the figure, which may give a better sense of the actual bias in the corrections. In NU 2-2001, bias is defined as the absolute value of the deviations ($\Delta r_{i,j}$). Over the clinical range of the scanner (the peak NEC activity [$a_{NEC,peak}$] and below), the maximum bias is less than 8.5% and the average bias is less than 4%.

Image Quality

Placement of the sphere, lung, and background ROIs on the transaxial slices of the phantom is shown on Figure 5. Figure 6A presents transverse image slices through the plane of the spheres both for sphere-to-background contrast

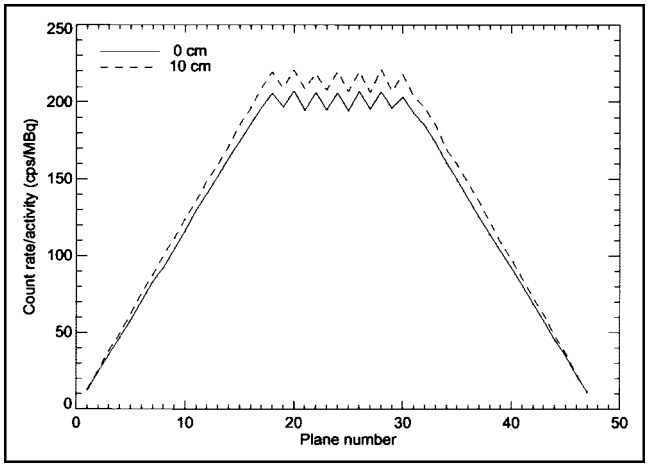

FIGURE 3. Axial sensitivity profile at the center of the FOV and at 10 cm off center.

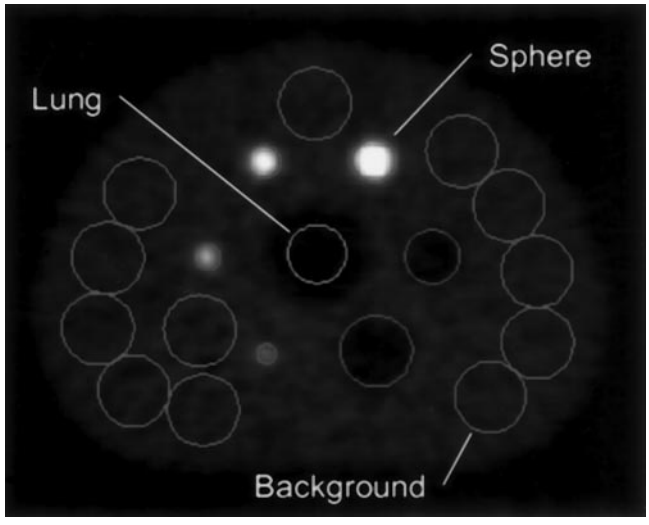

FIGURE 5. A transverse slice through the sphere phantom showing placement of the ROIs used for the analyses.

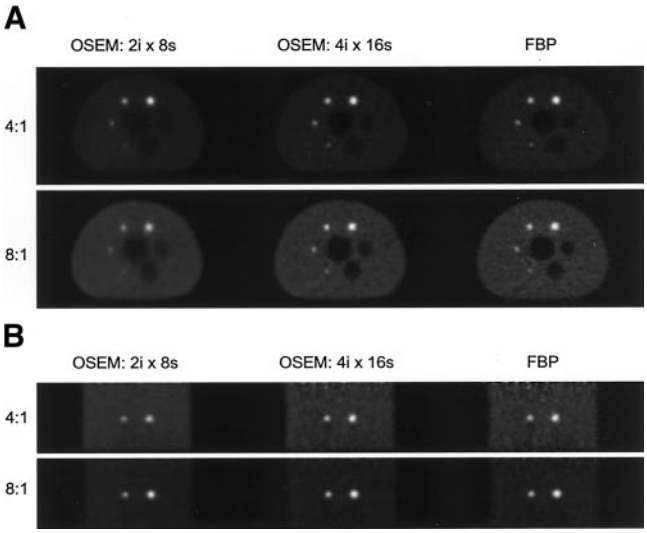

FIGURE 6. (A) The central-slice images of the image quality measurement. Top row: 4:1 contrast ratio. Bottom row: 8:1 contrast ratio. For each contrast, reconstructions using 3 common algorithms are shown. (B). Coronal slices through the 17- and 22-mm spheres, for each contrast ratio and reconstruction algorithm.

ratios and for each of the 3 reconstructions evaluated (negative values are truncated in the FBP images). Corresponding coronal slices through the 17- and 22-mm spheres are shown in Figure 6B. The dependence of contrast and noise level on the reconstruction algorithm can be observed. Tables 3 and 4 present our results for the sphere contrast ratios and background variabilities computed from these images, for the nominal 4:1 and 8:1 activity ratios, respectively. The results presented in these tables are based on the assayed values for the hot-to-background-activity ratios (3.99 and 8.17, Table 1). The uncertainties in these ratios imply corresponding uncertainties in the resulting hot sphere contrasts on the order of $\pm 10\%$

For these data, the results for OSEM with 4 iterations and 16 subsets were similar to those for FBP, both in contrast recovery and in background variability. OSEM with 2 iterations and 8 subsets gave considerably smoother images with correspondingly reduced contrast. The most appropriate algorithm for clinical applications is not entirely obvious and may, in fact, depend on the patient's characteristics (e.g., weight) as well as the task to be performed, such as lesion detection, tumor staging, or radiation therapy planning. It should also be noted that background variability does not reflect noise correlations and streak artifacts. To address this concern, the images were examined visually, and we did not find any discrepancies.

The results for the repeatability measurement of the contrast at the 8:1 ratio (Table 4) indicated that, except for the largest sphere, these values were repeatable to within 2%–4%. No systematic trend in contrast versus activity was observed for these. The largest sphere, on the other hand, exhibited a monotonic increase in contrast value with activity and a much higher relative deviation than did the other sphere. The reason for this is not yet understood.

Figures 7A and 7B show the value of the lung residual ($\Delta C_{lung,\,i}$) for each slice, for the 4:1 and 8:1 contrast ratios, respectively. For each contrast, results for the 3 reconstructions are plotted in percentage units. Because of the construction of this phantom, its active region does not extend beyond plane 42 of the LSO PET/CT when positioned according to NU 2-2001, resulting in the drop in residuals at higher plane numbers. It can be observed that there is a strong dependence of the residual values on the reconstruction algorithm used, although the scatter and attenuation corrections are the same in all cases. The mean residuals over planes 1–42 are given in Tables 3 and 4. Although the average error in the case of FBP reconstruction was very close to 0, there was significant bias in the iterative reconstructions, probably as a result of incomplete convergence in this large cold region. The plane-to-plane variability of the residuals was likely the result of statistical fluctuations. We observed similar variance across planes in a background ROI equal in size to the lung region. Thus, in our data, the residual deviations shown in Figures 7A and 7B appeared to measure primarily noise and reconstruction convergence

TABLE 3
Percentage Contrast, Background Variability, and Average Lung Residual for $n = 4$

Sphere size (mm)	Contrast (%)			Background variability (%)		
	2i × 8s*	4i × 16s†	FBP	2i × 8s*	4i × 16s†	FBP
10	12	22	22	3.5	6.2	8.1
13	17	29	29	3.2	5.3	6.4
17	29	38	38	2.9	4.4	4.7
22	41	48	48	2.8	3.8	3.6
28	45	60	67	2.7	3.4	3.0
37	51	62	66	2.6	3.1	2.7
Lung (average relative error)	31	13	0			

*Two iterations and 8 subsets.
†Four iterations and 16 subsets.

TABLE 4
Percentage Contrast, Background Variability, and Average Lung Residual for $n = 8$

Sphere size (mm)	Contrast (%)			Background variability (%)		
	2i × 8s*	4i × 16s†	FBP (relative deviation)	2i × 8s*	4i × 16s†	FBP
10	15	25	25 (3.3)	5.1	7.4	8.7
13	24	34	32 (2.3)	5.0	6.6	7.2
17	36	43	42 (4.0)	4.8	6.0	6.0
22	48	53	51 (1.7)	4.7	5.5	5.4
28	46	62	71 (3.5)	4.6	5.2	4.9
37	44	55	56 (11)	4.5	4.9	4.2
Lung (average relative error)	32	13	0			

*Two iterations and 8 subsets.
†Four iterations and 16 subsets.

errors, not errors in scatter and attenuation correction as was intended by NEMA. We suggest that users exercise care in interpreting the results of this so-called test for attenuation and scatter correction.

DISCUSSION

The aim of this study was to provide objective system performance measurements for the CPS LSO PET/CT scanner using the new NEMA NU 2-2001 performance measurement standards. Overall, with the exception of the image quality test, we found that these procedures were simpler to perform than the NU-1994 measurements and hence less time consuming. On the other hand, because the new tests were performed with longer and heavier phantoms, they required the help of a second physicist/technologist for setting up and prepositioning.

The new standards also incorporate the contribution of out-of-field activity in both the counting rate and image quality tests, which is reflected in the increased scatter fraction for a 3D-only system. These new tests attempted to approximate more realistic clinical conditions for whole-body scanning than did the NU 2-1994 standard. Although the new standards are partially successful in this attempt, we find some limitations as well, particularly with regard to the relationship between image quality, NECR, and injected patient dose. Thus, although they certainly provide useful information to the user or the scanner manufacturer and make it possible to compare systems from different vendors, we believe they do not accurately reflect clinical performance in most whole-body studies (*8*,*9*).

CONCLUSION

On LSO-based scanners it is not possible to follow the NU 2-2001 standard as written because of the nature of the intrinsic background radioactivity. Modifications to the procedures are needed for the scatter fraction, counting rate, and sensitivity tests. We have followed the recommendations of the scanner's manufacturer in performing these tests and found that, with appropriate adjustments in acquisition and processing methods, the NEMA tests can still be used to accurately evaluate such systems.

ACKNOWLEDGMENTS

We wish to thank the following individuals at CPS Innovations: James Bland for providing resources for these measurements, Dr. William C. Howe for providing valuable assistance with performing image quality analysis, Don Powers for constructing the point sources used for the resolution measurements, and Dr. Bernard Bendriem for useful discussions.

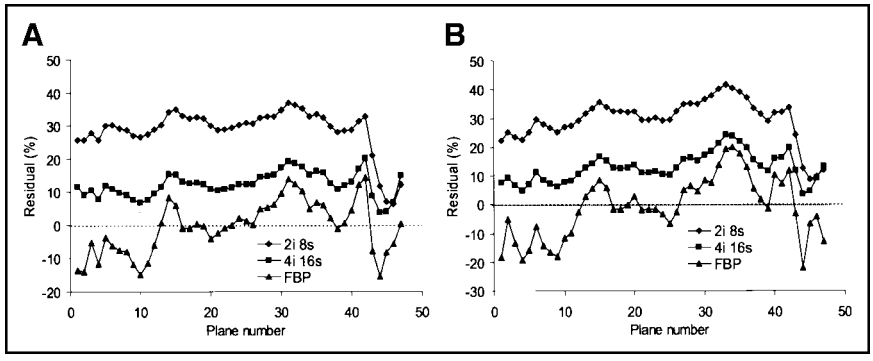

FIGURE 7. The relative lung residual (ΔC_{lung}) in percentage units, for each slice. (A) 4:1 contrast ratio. (B) 8:1 case contrast ratio.

REFERENCES

1. Nahmias C, Nutt R, Hichwa RD, et al. PET tomograph designed for 5-minute routine whole body studies [abstract]. *J Nucl Med.* 2002;43(suppl):11P.
2. Nutt R. Is LSO the future of PET? *Eur J Nucl Med Mol Imaging* 2002;29:1523–1525.
3. National Electrical Manufacturers Association. *NEMA Standards Publication NU-2 2001: Performance Measurements of Positron Emission Tomographs.* Rosslyn, VA: National Electrical Manufacturers Association; 2001.
4. National Electrical Manufacturers Association. *NEMA Standards Publication NU-2 1994: Performance Measurements of Positron Emission Tomographs.* Washington, DC: National Electrical Manufacturers Association; 1994.
5. Daube-Witherspoon ME, Karp JS, Casey ME, et al. PET performance measurements using the NEMA NU 2-2001 standard. *J Nucl Med.* 2002;43:1398–1409.
6. Watson CC, Casey ME, Eriksson L, Mulnix T, Adams D, Bendriem B. NEMA NU 2 performance tests for scanners with intrinsic radioactivity. *J Nucl Med.* 2004;45:822–826.
7. Watson CC, Casey ME, Bendriem B, et al. A new method for assessing and optimizing clinical ^{18}F-FDG whole-body PET data quality [abstract]. *J Nucl Med.* 2003;44(suppl):110P.
8. Watson CC, Casey ME, Beyer T, Bruckbauer T, Townsend DW, Brasse D. Evaluation of clinical PET count rate performance. *IEEE Trans Nucl Sci.* 2003; 50:1379–1385.
9. Badawi R, Adam L-E, Zimmerman RE. A simulation-based assessment of the revised NEMA NU-2 70-cm long test phantom for PET. In: *NSS and MIC Conference Record.* Vol. 3. San Diego, CA: IEEE; 2001:1466–1470.